SLAC-PUB-2788
August 1981
(A)

RELATIONSHIP OF FEL PHYSICS TO ACCELERATOR PHYSICS*

P. L. Morton
Stanford Linear Accelerator Center
Stanford University, Stanford, California 94305

I. INTRODUCTION

The main purpose of this talk is to describe the Free Electron Laser (FEL) in terms that are familiar to accelerator physicists. Since many of you are not accelerator physicists some discussion will be included to describe how an accelerator works. Once the similarity between the design and operation of an accelerator and a FEL is understood it will be possible to use the methods of accelerator design to assist us in the understanding and design of FEL's.

Shortly after the first successful operation of the FEL at Stanford[1] the first conference in this series was held in 1977 at Telluride.[2] This conference was extremely valuable in conveying much of the information about free electron lasers to the rest of the community. From these Telluride

* Work supported by the Department of Energy, contract DE-AC03-76SF00515.

(Presented at the FEL Workshop, Sun Valley, Idaho, July 13, 1981; also to be published in Physics of Quantum Electronics.)

lectures it was clear that it is possible to describe the FEL with a classical theory,[3] and for many cases it is possible to use a single electron analysis.[4] The following summer (1978) in La Jolla the results from the first Telluride Conference were used to study the FEL with a formulation developed for the design and operation of high energy accelerators and storage rings.[5] By the time of the next Telluride Conference in 1979,[6] accelerator terms were in wide use in many of the presented papers. Before describing what an FEL is and how it works let us begin by reviewing some properties of accelerators and storage rings.

II. REVIEW OF RELEVANT ACCELERATOR PROPERTIES

In a circular accelerator it is possible to define a closed or "equilibrium" orbit, which is a function of particle energy, such that if a particle is launched on this orbit at one point in the ring it will return to the same point in the ring traveling in the same initial direction. Generally there is only one such closed orbit for each particle energy. Two such equilibrium orbits are shown in Fig. 2.1, one for energy γ (measured in terms of the particle rest mass) and the second for energy $\gamma + \delta\gamma$.

The separation of the equilibrium orbits for different energies is given by $\delta x = \eta(\delta\gamma/\gamma)$, where η, a function of azimuth in the accelerator, is called the dispersion. The difference between the total path length of two different energy equilibrium orbits is given by

$$\frac{\delta L}{L} = \frac{\alpha}{\beta^2}\left(\frac{\delta\gamma}{\gamma}\right) \tag{2.1}$$

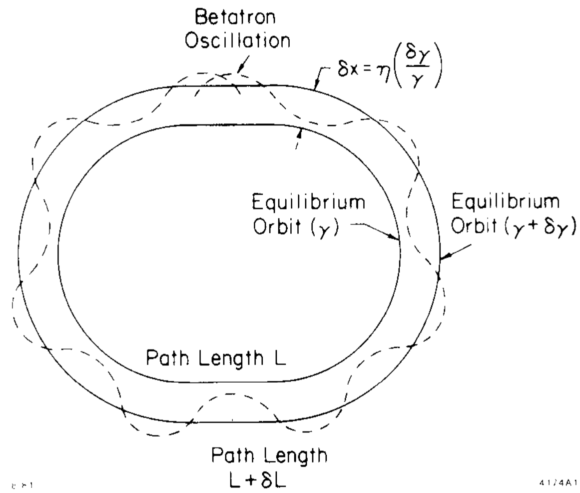

Fig. 2.1. Display of equilibrium orbits for various energies.

where α is an integral around the azimuth called the momentum compaction factor. The integral involves the η-function and the local bending radius. When particles are not initially on their equilibrium orbit, appropriate to their energy, they perform "betatron" oscillations about the equilibrium orbit as shown in Fig. 2.1.

Since both the speed (v) and the path length (L) depend upon particle energy (γ) the change in the total angular revolution frequency (ω_0) is given by

$$\frac{\delta\omega_o}{\omega_o} = \left(\frac{\delta v}{v} - \frac{\delta L}{L}\right) \tag{2.2}$$

which may be written as

$$\frac{\delta\omega_o}{\omega_o} = \frac{1}{\beta^2}\left(\frac{1}{\gamma^2} - \alpha\right)\frac{\delta\gamma}{\gamma} \tag{2.3}$$

We see that at a particular energy denoted as the transition energy, $\gamma_t = \alpha^{-1/2}$, the increase in particle speed with energy is exactly compensated by the increase in path length with energy. Now consider the case where an electric field in an rf cavity in the ring is oscillating at harmonic (h) of the nominal angular revolution frequency (ω_0). We find that the average change in the phase (ψ) of the electric field in the cavity between the time of successive passages of the particle through the cavity is given by

$$\frac{d\psi}{dz} = \frac{(\Delta\psi)_{\text{one revolution}}}{2\pi R} = -\frac{h}{\beta^2 R}\left(\frac{1}{\gamma^2} - \alpha\right)\frac{\delta\gamma}{\gamma} \tag{2.4}$$

where R is the average ring radius equal to the circumference divided by 2π, and z is a coordinate measured along the nominal equilibrium orbit. We see that the rate of the phase change with energy is determined by a change in both the particle velocity and the path length traveled along the closed orbit.

In order to accelerate particles in an accelerator we use rf cavities to produce an electric field in the longitudinal direction of the particle motion. Two such cavities are shown in Fig. 2.2 separated by a distance L. In such cavities the sense and magnitude of the electric field oscillate with time. When the electric force is in the same direction as the particle velocity the particle is accelerated and the electric field has transfered energy to the particle. Conversely, if the electric force opposes the velocity of the particle the particle is decelerated and energy is transferred to the electric field. Thus accelera-

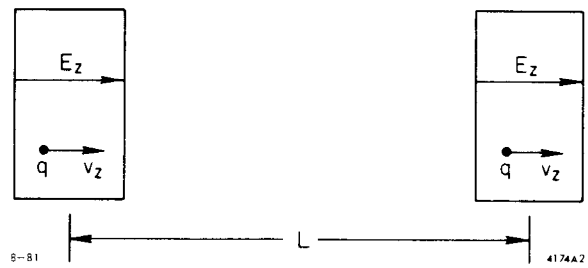

Fig. 2.2. Illustration of acceleration with rf cavities.

tion or deceleration depends upon the relative phase between the longitudinal velocity vector v_z and the longitudinal electric field vector E_z at the time when the particle passes through the cavity. The rate of change in the particle energy may be written as

$$\frac{d\gamma}{dz} = \frac{q\langle E_z\rangle}{mc^2} \sin \psi \tag{2.5}$$

where q is the particle's charge, mc^2 the rest mass energy of the particle, $\langle E_z\rangle$ the magnitude of the average electric field the particle experiences in traveling distance dz, and ψ is the relative phase between the longitudinal electric force vector and the longitudinal particle velocity vector defined above.

In particle accelerators the arrangement of accelerating cavities can vary widely. In a linac many cavities are arrayed in a straight line and the particles pass through each of them once. In a circular accelerator there may be one or several cavities and the particles pass through all of them on each revolution. For our present purpose let us presume we are dealing with a circular accelerator with only one accelerating cavity so that L is the circumference of the nominal equilibrium orbit. In this case, there is a synchronous (resonant) phase ψ_r between the velocity v_z and the electric field E_z of the cavity at which a particle will gain or lose exactly the proper energy to remain synchronous. The synchronous phase obeys the equation

$$\frac{d\gamma_r}{dz} = \frac{q\langle E_z\rangle}{mc^2} \sin \psi_r \ . \tag{2.6}$$

By defining the energy deviation $\delta\gamma = \gamma-\gamma_r$ we obtain the following differential equation for the energy deviation of a particle which is not riding at the synchronous phase.

$$\frac{d(\delta\gamma)}{dz} = \frac{q\langle E_z\rangle}{mc^2} \left(\sin \psi - \sin \psi_r\right) \ . \tag{2.7}$$

The differential equation for the phase (ψ) is given by Eq. (2.4). Equations (2.4) and (2.7) are the standard rf equations used by accelerator designers for years and a great deal of work has been done in analyzing these equations.[7] Later we will demonstrate the similarity between these equations and those which describe the FEL and show how the analysis of accelerator designers may be used for FEL design.

For the case where the changes in the parameters are adiabatic we can immediately draw the trajectories in phase space which correspond to the solutions of Eqs. (2.4) and (2.7). These trajectories are shown in Fig. 2.3 for particles with energies below transition energy, and therefore with $\sin \psi_r > 0$. [For accelerator designers the synchronous phase reference is chosen such that below transition energy the synchronous particle is accelerated when

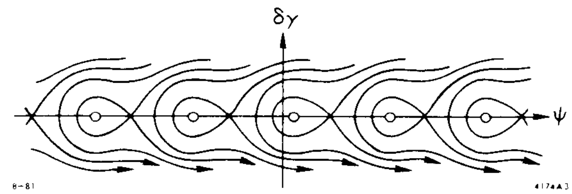

Fig. 2.3. Trajectories in ψ, $\delta\gamma$ phase plane for $\psi_r > 0$ below transition energy.

$0 < \psi_r < \pi/2$. This custom is in accordance with Eq. (2.6).] The closed trajectories correspond to particles trapped in buckets and which perform stable "synchrotron" oscillations about the resonant phase and energy. The maximum stable phase curve of a single bucket is shown in Fig. 2.4. The maximum value of $\delta\gamma$ for which a particle may be trapped in a bucket is given by

$$\delta\gamma_m = \left[\frac{2\beta^2 Rq\langle E_z\rangle\gamma}{hKmc^2}\right]^{1/2} \Gamma(\psi_r) \qquad (2.8)$$

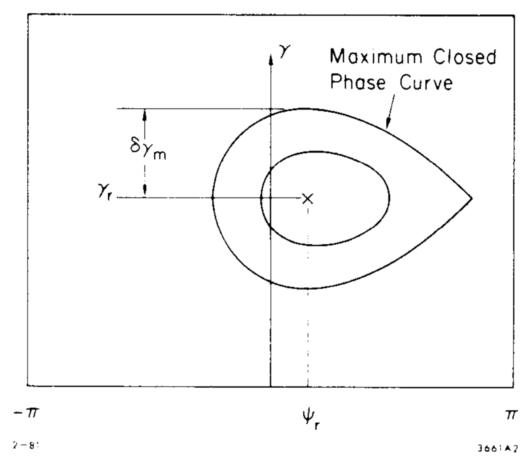

Fig. 2.4. Stable phase plane trajectories.

with

$$K = [\frac{1}{\gamma^2} - \alpha] \tag{2.9}$$

and

$$\Gamma(\psi_r) = [\cos \psi_r - (\frac{\pi}{2} \sin \psi_r - \psi_r) \sin \psi_r]^{1/2} \ . \tag{2.10}$$

We note that Γ varies between its maximum value of one (at $\psi_r = 0$) to zero (at $\psi_r = \pi/2$). Within the bucket small amplitude motion is nearly sinusoidal with a frequency of

$$\Omega_L = [\frac{hK\langle E_z\rangle \cos \psi_r}{\beta^2 \gamma R mc^2}]^{1/2} \ . \tag{2.11}$$

The terms spontaneous and stimulated emission are often used by laser physicists and it will be useful to illustrate how an accelerator physicist views these phenomena. Consider an empty rf cavity, at time $t < 0$, i.e., one where $E_z = 0$ for $t < 0$ (see Fig. 2.2). Let a particle of charge q enter the cavity with velocity v_z at time $t = 0$ and exit at time $t = t_1$. At time $t > t_1$ this charge will have excited a field in the cavity at various modes. For the λth mode this excited field may be written as

$$\bar{\vec{E}}_\lambda(\vec{r}) = q\, \bar{\vec{f}}(\vec{r}) \tag{2.12}$$

where $\bar{\vec{f}}(\vec{r})$ is independent of q, the bar over a quantity denotes a complex phasor at frequency ω_λ, and $\vec{r}$ is the position in the cavity. The phase of the longitudinal component of $\vec{\bar{f}}(\vec{r})$ is opposite to the phase of the particle velocity v_z. The stored energy in the λth cavity mode following the passage of the particle is independent of time (for a perfectly conducting cavity) and is given by

$$U = kq^2 \int \vec{\bar{f}}^{*}(\vec{r}) \cdot \vec{\bar{f}}(\vec{r})\, d\vec{r} \qquad (2.13)$$

where k is a constant of proportionality that depends on the units used.

If instead of a single particle traveling through the rf cavity we imagine a continuous uniform beam we find that we have a superposition of fields from many particles all at separate phases. The sum of all of these separate fields would be zero (if we ignored the effect of the field from one particle acting on another particle). Thus for a beam of particles to excite or leave behind stored energy in the cavity it is necessary to have a density fluctuation in the beam at the resonant mode frequency of the cavity. This fluctuation may be noise due to statistical, quantum, or other sources. A plot of the response of the cavity as a function of the frequency of the density variation is given by Fig. 2.5. A laser physicist would call this "the gain curve for spontaneous emission.

Next we consider this same rf cavity except we assume that at t = 0 there is an electromagnetic field present (see Fig. 2.2) given by

$$\vec{\bar{E}}_z = \vec{\bar{E}}_o(\vec{r}) \qquad (2.14)$$

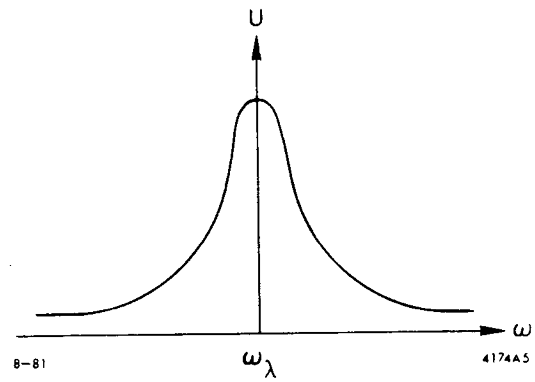

Fig. 2.5. Gain curve for spontaneous emission.

with an initial stored energy

$$U_o = k \int \vec{\bar{E}}_o^*(\vec{r}) \cdot \vec{\bar{E}}_o(\vec{r})\, d\vec{r} \; . \tag{2.15}$$

After the particle has left the cavity the electric field in the cavity is given by sum of the original field and the induced field, i.e.,

$$\vec{\bar{E}}_z = \vec{\bar{E}}_o(\vec{r}) + q\vec{\bar{f}}(\vec{r}) \tag{2.16}$$

and the stored energy is given by

$$U = U_o + 2kq \text{ Real Part } \left[\int \vec{\bar{E}}_o^*(\vec{r}) \cdot \vec{\bar{f}}(\vec{r})\, d\vec{r} \right]$$

$$+ q^2 k \int \vec{\bar{f}}^*(\vec{r}) \cdot \vec{\bar{f}}(\vec{r})\, d\vec{r} \; . \tag{2.17}$$

The change in the stored energy of the cavity is due to two terms. The second term on the rhs of Eq. (2.17) is the stimulated emission while the third term is the spontaneous emission discussed above.

It is possible to write the second or stimulated term, which represents the interference between the spontaneous induced electric field and the original electric field, as

$$\Delta U = - q \langle E_z \rangle \sin \psi \tag{2.18}$$

where ψ is minus the phase between the induced electric field (which opposes the longitudinal particle velocity) and the original electric field.

In other words the stimulated emission (or absorption for positive ψ) is just the transfer of energy from the particle as it is decelerated (or accelerated) and depends upon the relative phase between the particle's longitudinal velocity v_z and the electric field in the cavity. Usually the stimulated emission is much larger than the spontaneous emission and we can treat the total effect as if a charged particle is decelerated (or accelerated) by the electromagnetic field in the cavity.

III. DESCRIPTION OF A FEL

A free electron laser consists of a wiggler field through which a beam of electrons passes, together with a plane electromagnetic wave as shown in Fig. 3.1. The wiggler field may be either a periodic magnetic bending field or a different electromagnetic wave traveling in the opposite direction. Laser people refer to this wiggler field as the pump field. For simplicity we will restrict our consideration only to periodic magnetic wiggler fields. The electrons enter the wiggler at $\gamma(0)$ and leave the

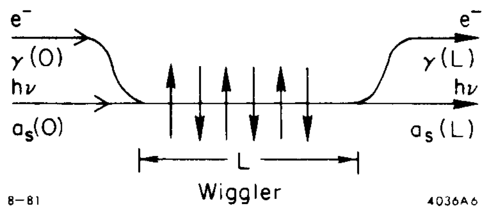

Fig. 3.1. Schematic representation of free-electron-laser.

wiggler with energy $\gamma(L)$, while the intensity of the electromagnetic radiation enters with an initial value $a_s(0)$ and exits with a value $a_s(L)$. For FEL operation it is important that energy from the electron beam be transferred to the electromagnetic radiation, i.e.,

$$\gamma(L) < \gamma(0) \quad \text{and} \quad a_s(L) > a_s(0) \ .$$

There are two operating regimes for the FEL. The first, called the Raman regime, is characterized by collective interactions between the electrons being important, and occurs for high electron beam currents and low electron energy ($\gamma \sim 1$). The second, called the Compton regime, is the single particle regime where collective effects may be ignored, and occurs for large values of electron energy ($\gamma > 10$).

The FEL is classified as an amplifier if the electromagnetic wave passes through the FEL only once. For this mode of operation to be useful it is necessary to have a high gain, i.e., $a_s(L) >> a_s(0)$. If mirrors are used to recirculate the photons then the FEL is classified as an oscillator and low gain devices in which $a_s(L) \tilde{>} a_s(0)$ are useful.

Similarly we can use a linac to produce a beam of electrons which pass through the FEL only once or use a storage ring to recirculate the electron beam so the same electrons pass through the FEL many times.

One of the important differences between the accelerating cavity described above and the FEL is, that the electric field in the accelerating cavity is in the longitudinal direction of the electron beam motion while the electric field of the FEL is in the transverse direction perpendicular to the longitudinal velocity of the electron beam. In order for the electron and the optical electromagnetic field to exchange energy it is necessary for the electron to have a velocity in the same direction as the transverse electric field of the optical wave. One method of obtaining this transverse velocity is by the use of a wiggler magnetic field. A wiggler magnet is one with a transverse magnetic field which oscillates in amplitude as a function of the longitudinal coordinate. There are two types of wigglers; the helical type as originally used by Madey to amplify circularly polarized light and the linear wiggler which amplifies linearly polarized light. An example of an linear wiggler and the transverse particle motion is shown at the top of Fig. 3.2. The magnetic field is given by

$$B_y = \sqrt{2}\, B_o \sin k_w z \tag{3.1}$$

with B_o the rms magnetic field strength and $\lambda_w = 2\pi/k_w$ the wiggler wavelength. The transverse angle of the oscillation in such a wiggler is given by

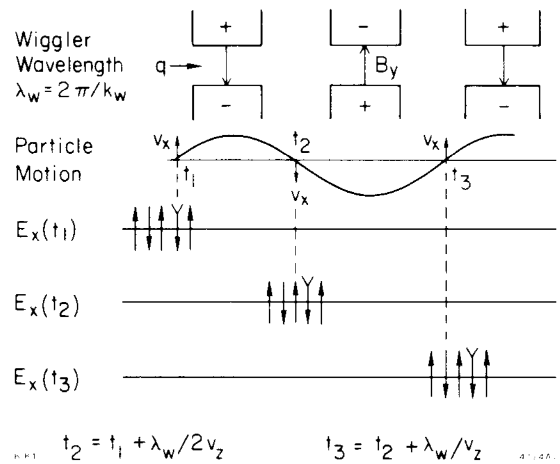

Fig. 3.2. Interaction of electron transverse velocity with transverse electric force of optical electromagnetic wave at various times and positions in FEL.

$$x' = \frac{v_x}{v_z} = \frac{a_w}{\gamma} \cos k_w z \tag{3.2}$$

where a_w is the reduced wiggler vector potential

$$a_w = \frac{e B_o}{k_w mc^2} \tag{3.3}$$

and we have neglected the explicit dependence of the transverse electron motion upon the optical electromagnetic field. This last approximation is quite good; for example, a 1 μm laser with an intensity of 10 Gwatt/cm^2 has a less-than-one-part-in-10^4 effect on the transverse electron velocity.

In Fig. 3.2 we display the mechanism for the transfer of energy between the electron and the transverse electric field of the optical plane wave. We consider an electron in the wiggler at time t_1 with its transverse velocity v_x

positive as shown in Fig. 3.2. At time $t_2 = t_1 + \lambda_w/2v_z$ the electron has traveled along the wiggler one-half of a wiggler period and the sign of v_x has changed, while at time $t_3 = t_1 + \lambda_w/v_z$ the electron has traveled one full wiggler period and v_x is positive. The electric force from the optical wave is represented by arrows displayed in Fig. 3.2 labeled E_x for the various times. Notice that at time t_1 the electric force from the optical wave opposes the transverse velocity v_x of the electron. This electric force arrow is marked with a large tail. We consider the case where the optical wavelength is chosen such that at time t_2 the optical wave has traveled one-half of an optical wave further in the longitudinal direction than the electron beam. The new electric force vector is now one-half wavelength behind the original electric force vector (with the tail) and opposes the new transverse electron velocity. Similarly at time t_3 the optical wave has moved ahead of the electron by one full optical wavelength and again the electric force opposes the transverse electron velocity. For the transverse electron velocity to remain in phase with the optical force the electron slips behind the optical wave by one optical wavelength in traveling one wiggler period. This is the condition for resonance where, on the average, the electron will either give or receive energy from the optical field depending upon the initial phase between the transverse electron velocity and the electric force of the optical wave.

The distance the electron slips behind the optical wave is due to two effects. The first effect results from the fact that speed v of the electron is less than the phase velocity c of the optical wave. The second effect occurs because in one wiggler period, the path length (L) traveled by the electron is greater than the distance (λ_w) traveled by the optical wave. Note that the change in the phase of the transverse electron velocity equals 2π in one wiggler period (Fig. 3.2). The net rate of change in the phase between the transverse electron velocity and the optical electric force is therefore given by

$$\frac{d\psi}{dz} = \frac{2\pi}{\lambda_w} - \frac{2\pi}{\lambda_s}\left(\frac{c - v}{v} + \frac{L - \lambda_w}{\lambda_w}\right) \tag{3.4}$$

where λ_s is the optical wavelength. We use the approximate relationships

$$\frac{L - \lambda_w}{\lambda_w} \approx \frac{1}{2}\overline{(x')^2} \tag{3.5}$$

and $c-v \approx c/2\gamma^2$, to obtain

$$\frac{d\psi}{dz} = k_w - \frac{k_s}{2\gamma^2}\left(1 + a_w^2\right) \tag{3.6}$$

where we have used $\overline{(x')^2}$ to indicate the average of $(x')^2$ over one wiggler period, Eq. (3.2) for x', and k_s is the optical wave number $= 2\pi/\lambda_s$. The resonance condition is given by $d\psi/dz = 0$ or

$$\lambda_s = \frac{\lambda_w}{2\gamma_r^2}\left(1 + a_w^2\right) . \tag{3.7}$$

The subscript r on γ indicates the value of the electron energy (designated as the resonance energy) for which the resonance relationship between λ_s and λ_w exists.

For electron energies different from the resonance energy the phase (which we designated by ψ) between the transverse electric velocity and the optical electric force is no longer constant, and its rate of change is given by

$$\frac{d\psi}{dz} = k_s \left(\frac{\delta v}{v} - \frac{\delta L}{L}\right) \tag{3.8}$$

where $k_s = 2\pi/\lambda_s$ is the optical wave number.

$\delta v/v$ is the change in electron speed due to the energy difference.

$\delta L/L$ is the change in the path length traveled by electron due to the energy difference.

The difference between trajectories for an electron at energy γ_r and for an electron with $\gamma = \gamma_r + \delta\gamma$ is shown in Fig. 3.3. The higher energy electron travels a shorter path (opposite to the usual case for circular accelerators) by an amount

$$\delta L = \delta \int ds \approx \frac{1}{2} \delta \int (x')^2 \, dz \, . \tag{3.9}$$

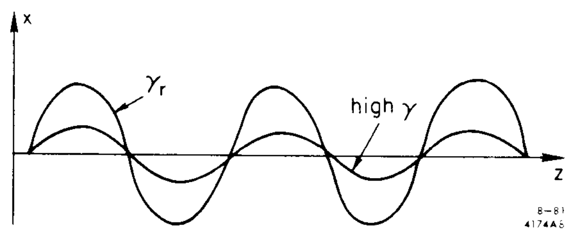

Fig. 3.3. Trajectories for electrons with different energies.

Using the expression for x', Eq. (3.2), we have

$$\frac{\delta L}{L} = -\left(\frac{a_w^2}{\gamma_r^2}\right) \frac{\delta\gamma}{\gamma} \, . \tag{3.10}$$

The higher energy electron also has a higher speed given by

$$\frac{\delta v}{v} = \left(\frac{1}{\gamma_r^2}\right) \frac{\delta\gamma}{\gamma} . \qquad (3.11)$$

Thus the equation of motion for the change in the phase difference between the transverse electron velocity and the optical electron field is given by

$$\frac{d\psi}{dz} = k_s\left(\frac{1}{\gamma_r^2} + \frac{a_w^2}{\gamma_r^2}\right) \frac{\delta\gamma}{\gamma} . \qquad (3.12)$$

Except for a sign difference in the definition of ψ this expression may be compared to the equation of motion for the rf phase variable used in accelerator theory [Eq. (2.4)]. We see that the FEL has a negative momentum compaction factor [see Eq. (2.1)]; this mean that no special or transition energy exists for which the increase in electron velocity with energy is compensated by a change in the path length with energy. This is an important difference as we will see when we discuss the gain-expanded FEL. It is possible to use the resonance definition for ψ [Eq. (3.7)] to rewrite Eq. (3.12) as

$$\frac{d\psi}{dz} = 2k_w \left(\frac{\delta\gamma}{\gamma}\right) . \qquad (3.13)$$

Now the change in the energy of the electron is proportional to the transverse velocity of the electron, the transverse electric field of the wave, and the sine of the relative phase ψ, so we can write the equation of motion for this energy change as

$$\frac{d\gamma}{dz} = \gamma' = -\frac{k_s a_s a_w}{\gamma} \sin\psi \qquad (3.14)$$

where

$$a_s = \frac{e(E_x)_{rms}}{k_s\ mc^2} \ . \qquad (3.15)$$

We define the relationship between the resonant phase (ψ_r) and the resonant energy (γ_r) by

$$\gamma_r' = -\frac{k_s\ a_s\ a_w}{\gamma_r} \sin\psi_r \ . \qquad (3.16)$$

Then defining $\delta\gamma = \gamma - \gamma_r$ we can obtain the following equation of motion.

$$\frac{d(\delta\gamma)}{dz} = -\frac{k_s\ a_s\ a_w}{\gamma_r}\left(\sin\psi - \sin\psi_r\right) \ . \qquad (3.17)$$

For the FEL, Eqs. (3.13) and (3.17) describe the same type of motion about the resonant energy as is described by Eqs. (2.4) and (2.7) for the synchrotron motion in accelerators. The phase space motion of the electron in an FEL may therefore be described by the same phase space curves as displayed in Figs. 2.3 and 2.4.

We make the transfer from the synchrotron equations of motion used in accelerator design to those used in FEL design by

$$\frac{q\langle E_z\rangle}{mc^2} \rightarrow -\frac{k_s\ a_s\ a_w}{\gamma_r} \qquad (3.18)$$

and

$$-\frac{h}{\beta_r^2 R}\left(\frac{1}{\gamma_r^2} - \alpha\right) \rightarrow k_s\left(\frac{1}{\gamma_r^2} + \frac{a_w^2}{\gamma_r^2}\right) = 2k_w \ . \qquad (3.19)$$

When these relations are substituted into the accelerator synchrotron equations for the bucket parameters, Eqs. (2.8) and (2.11), we obtain

$$\left(\frac{\delta\gamma_m}{\gamma}\right) = 2\left[\frac{a_s a_w}{1 + a_w^2}\right]^{1/2} \Gamma(\psi_r) \qquad (3.20)$$

for the maximum energy excursion contained in the bucket, and

$$\Omega_L = 2k_w \left[\frac{a_w\ a_s \cos\psi_r}{1 + a_w^2}\right]^{1/2} . \qquad (3.21)$$

for the frequency of small amplitude energy oscillations. By combining these equations we may rewrite Eq. (3.21) as

$$\Omega_L = k_w \frac{[\cos\psi_r]^{1/2}}{\Gamma(\psi_r)} \left(\frac{\delta\gamma_m}{\gamma}\right) . \qquad (3.22)$$

The use of buckets to describe the electron synchrotron motion in the FEL has been presented in many other places,[5-6] but because of the importance of this concept as well as for completeness we will present the work again in this paper.

IV. CONSTANT PARAMETER WIGGLER

The "standard operational mode" of the FEL, which was the mode used in the Madey experiment, is one in which the wiggler wave number k_w and field amplitude a_w are constant. The resonant energy γ_r is therefore also constant, and the resonant phase $\psi_r = 0$. From Eq. (3.7) we have

$$\gamma_r^2 = k_s\left(\frac{1 + a_w^2}{2k_w}\right) . \qquad (4.1)$$

In this mode the buckets are nonaccelerating or stationary. At first glance it is a little difficult to understand how such a device can work since the energies of electrons injected near the resonant energy with a uniform phase distribution will oscillate about the resonant energy (which remains constant). The key to successful operation of the FEL in this mode is to inject the electrons above the resonant energy and to allow them to complete only a fraction of an oscillation, as shown in Fig. 4.1.

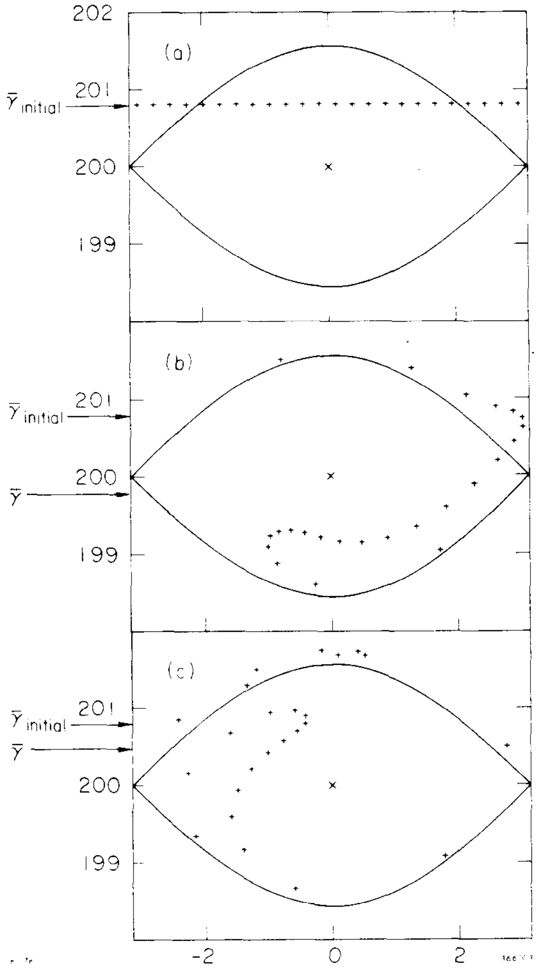

Fig. 4.1. Evolution of the electron energy distribution: (a) initial distribution; (b) after one-half oscillation; and (c) after nearly one-oscillation.

The electrons with either large or small energy deviations (compared to $\delta\gamma_m$) will have only a small average energy change, while electrons with an initial energy deviation $\delta\gamma_i \sim \delta\gamma_m$ and which perform approximately one-half of an oscillation will have their average energy reduced the most. For maximum gain it is important to choose both the initial energy and the wiggler length correctly. Figure 4.2 shows how for a fixed wiggler length, the energy extracted from the beam depends upon the initial energy.

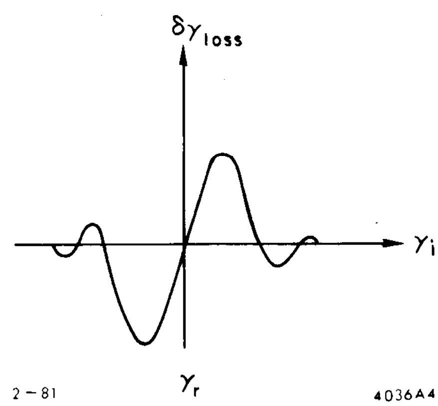

Fig. 4.2. Gain curve for stimulated emission. Energy loss of electrons versus initial energy or signal frequency.

It is clear that either we can regard the electron energy as the quantity which differs from its resonant value or we can regard the signal frequency ($\omega_s = k_s c$) as the quantity which differs from its resonant value. The relation relating these two viewpoints is

$$\frac{\delta\omega_s}{\omega_s} = 2\left(\frac{\delta\gamma}{\gamma}\right) . \tag{4.2}$$

Therefore, Fig. 4.2 may also be regarded as a plot of the signal intensity increase as a function of the signal frequency. The width of this "gain" curve is of the order of the bucket height $(\delta\gamma_m/\gamma)$, so that for a beam of electrons with an initial energy spread much larger than the bucket height, only a small fraction will transfer energy to the optical wave. We see from Fig. 4.1 and Eq. (3.20) with $\psi_r = 0$ that the maximum energy loss by the electrons is given by

$$\left(\frac{\delta\gamma}{\gamma}\right)_{\text{max loss}} \sim \left(\frac{\delta\gamma_m}{\gamma}\right) = 2\left[a_s a_w/(1 + a_w^2)\right]^{1/2} \tag{4.3}$$

while electrons emerge from the wiggler with an energy spread

$$\left(\frac{\delta\gamma}{\gamma}\right)_{\text{spread}} \sim \left(\frac{\delta\gamma_m}{\gamma}\right) . \tag{4.4}$$

The optimum wiggler length for maximum energy transfer from the electrons to the signal wave follows from Eq. (3.22)

$$L = \frac{\pi}{\Omega_L} = \frac{\lambda_w}{2(\delta\gamma_m/\gamma)} . \tag{4.5}$$

When this equation is combined with Eq. (4.3) we find that the maximum energy that can be extracted from the electrons in this mode of operation is given by the simple relationship

$$\left(\frac{\delta\gamma}{\gamma}\right)_{\text{max loss}} \sim \frac{1}{2N} \tag{4.6}$$

where N is the number of wiggler magnet periods. The fact that, for a constant parameter wiggler, the average energy spread produced by the FEL is always equal or greater than the average energy loss follows from a more general theorem proved by Madey.[8] This places a severe restriction on the efficiency of this type of FEL. Renieri[9] has shown that if such an FEL is operated in a storage ring, with the synchrotron radiation used to damp the energy spread due to the FEL, the maximum obtainable laser power is related to the power radiated into synchrotron radiation by

$$P_{laser} < 2P_{synch}\left(\frac{\delta\gamma_m}{\gamma}\right) . \qquad (4.7)$$

There are FEL-storage ring projects, which use the radiation damping to limit the energy spread of the electrons, at Orsay, Frascati, Brookhaven and Novosibirsk.

It should be noted that the equations of motion derived above are Hamiltonian, guaranteeing that the phase area is conserved. The net increase in the energy spread is due to a combination of phase area filamentation and a smearing of the optical phase angle as the electrons travel around the storage ring from the end of the FEL back to the entrance.

Deacon[10] has analyzed the operation of a constant parameter FEL in an isochronous storage ring. As an electron travels around the ring, such a device maintains the phase relationship between the electron and the optical wave. The electron is trapped in the optical bucket and can transfer energy from the low frequency rf cavity to the high frequency optical cavity. He discusses the design of a storage ring capable of restricting the spread in the longitudinal position of the electrons to be less than a fraction of the optical wavelength. This requires of the storage ring a very low momentum compaction factor, and consequently the longitudinal focusing is very weak in the absence of the optical wave. At the present time, this idea has not been explored experimentally.

V. VARIABLE PARAMETER WIGGLER SCHEMES

While it is gratifying to note that it is possible to use the graphic techniques of accelerator designers to derive the results of the constant parameter wiggler, the real advantage of establishing the relationship between the FEL physics and accelerator physics is that we can use the results of accelerator physics to design other types of FELs.

As our first example of an accelerator design which has been appropriated to design a new kind of FEL we consider the case of a standing wave linac (used for nonrelativistic particles) where the distance between consecutive accelerating cavities increases along the linac. By analogy it suggests the variable parameter wiggler. For this case the longitudinal velocity and hence also the energy of the resonant particle must increase along the linac in order for the particle to remain at a constant synchronous phase with respect to the longitudinal electric field of the cavity. We see from Eq. (2.6) that the synchronous phase(ψ_r) must be greater than zero and the average accelerating field $\langle E_z \rangle$ must be large enough to produce the necessary rate of energy gain. From Fig. 2.3 we see that the group of trapped particles, near the resonant particle in energy and phase, will be accelerated along with the resonant particle.

This scheme has been used in the design of a variable parameter wiggler for FEL operation by allowing the wiggler wave number (k_w) and the magnetic vector potential (a_w) to vary along the longitudinal direction of the wiggler. The main difference between this scheme and the standing-wave linac is that, in the FEL, rather than accelerate the electrons, we want to decelerate them and transfer energy to the optical wave. Equation (3.16) tells us that this is possible for $\psi_r > 0$. For a sufficiently large value of optical field intensity (a_s) electrons will be trapped in the decelerating optical bucket, and will have their average energy reduced by an amount equal to the decrease in the resonant energy.

$$\Delta\gamma_r = \left[\gamma_r(0) - \gamma_r(L_T)\right] \tag{5.1}$$

where L_T is the total length of the FEL. It follows from the resonance condition Eq. (3.7) that the change in the resonance energy is related to the change in the wiggler parameter by

$$\Delta\left(\gamma_r^2\right) = \frac{k_s}{2}\,\Delta\left(\frac{1 + a_w^2}{k_w}\right) . \tag{5.2}$$

There are many options in how to change a_w and k_w as functions of z to satisfy Eq. (5.2) for a desired variation of γ_r, several of which were discussed at the 1979 Telluride Conference. As we see from Fig. 5.1 only a portion of the electrons are trapped in the bucket and hence decelerated. The remaining untrapped electrons actually have their energy increased slightly so that the electrons will exit the FEL with a large spread in the energy. This large energy spread in the beam makes it difficult to reuse the electrons in the FEL again.

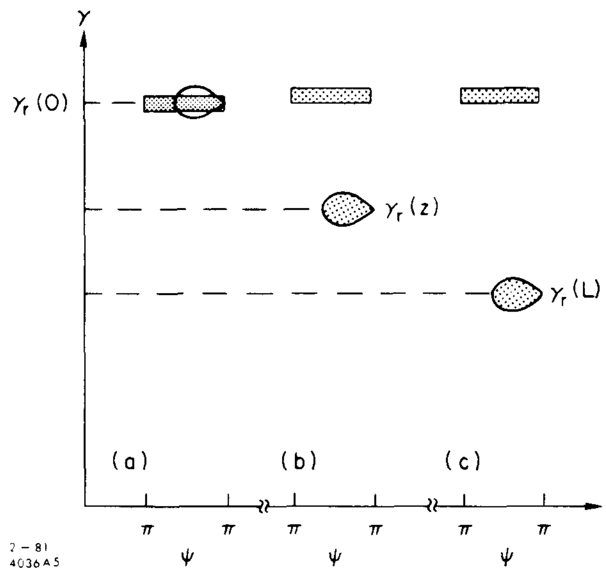

Fig. 5.1. Electron phase area distribution: (a) at the wiggler entrance; (b) at the wiggler center; and (c) at the wiggler exit.

At the present time in this country there are three experiments under way to study this mode of FEL operation. These experiments are located at TRW, LASL and Math. Sci. N. W. and they will be discussed later in this meeting.

In circular accelerators the method of adiabatic capture has been used to capture and accelerate nearly all of the injected particles in an rf bucket. This is accomplished by using a "stationary" bucket where $\psi_r = 0$, so that the bucket extends in phase from $-\pi$ to π, and by increasing the accelerating field E_z with time from an initial value of zero. In this method of operation we see that the bucket area increases from an initial value of zero as $[\langle E_z \rangle]^{1/2}$. If the rate of increase in the bucket area is slow enough [compared to the final value of the linear oscillation frequency Ω_L, Eq. (2.11)] and if the final bucket area is larger than the original phase area of the injected particles then nearly all of the particles will be trapped in the bucket and the final phase area occupied by the beam will be only slightly larger than its initial value.

After all of the particles are captured in the center of the stationary bucket, the guide field of the circular accelerator is increased so that the energy of the resonant particle must also increase to maintain resonance between the particle and the cavity. The resonant phase ψ_r then changes from zero to a positive value and the trapped particles are subsequently accelerated. The advantage of this scheme is that essentially all of the particles are trapped and accelerated, and the final energy spread of the particles is kept small.

As our second example where accelerator design has influenced the design of FELs we consider an analogous scheme of adiabatic capture, deceleration, and decapture that permits a reasonable reduction in the energy of all of the electrons while at the same time minimizing the increase in the energy spread of the electrons.[5] This scheme is shown in Fig. 5.2. To describe this process we divide the wiggler into five regions: Region 1, where adiabatic capture occurs; Region 2, where the average phase angle is changed; Region 3, where the deceleration occurs; Region 4, where the average phase angle decreases to zero; and Region 5, where the decapture occurs. In Region 1, we require

$$k_w(z) = \frac{k_s}{2\gamma_r^2}\left[1 + a_w^2(z)\right] \tag{5.3}$$

for γ_r constant equal to $\gamma_r(0)$ the average energy of the injected beam. As a_w is increased along the wiggler from zero at the entrance this relation ensures that ψ_r the resonance phase remains zero.

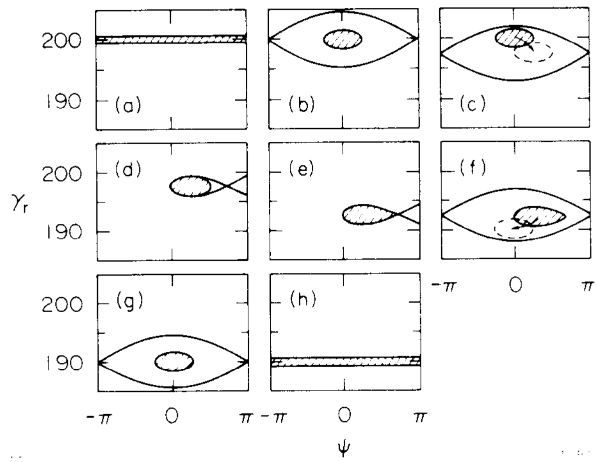

Fig. 5.2. Schematic behavior of the γ, ψ phase space distribution as a function of z during adiabatic capture, deceleration, and decapture processes: (a) initial distribution; (b) during capture; (c) during increase of average ψ; (d) and (e) deceleration process; (f) during the decrease of the average ψ; (g) during decapture; and (h) after decapture.

The injected electrons with a small initial energy spread centered at $\gamma_r(0)$ [see Fig. 5.2(a)] are captured into the stationary bucket by the adiabatically increasing height of the bucket. The bucket growth may be accomplished by increasing a_w from zero to a maximum value of one. If the initial energy spread of the beam is less than the final bucket area, i.e.,

$$2\pi\left(\frac{\delta\gamma}{\gamma}\right)_{\text{initial}} < 8\left[2a_s\right]^{1/2} \tag{5.4}$$

then with an adiabatic change of $a_w(z)$ the electrons become trapped in the center of the bucket [see Fig. 5.2(b)]. It follows from Eq. (5.3) that if a_w is held constant a small discontinuous increase in k_w at the beginning of Region 2 results in small discontinuous decrease in the resonant energy of the bucket. The average phase of the electrons will be increased from zero to a positive value in this new bucket as shown in Fig. 5.2(c).

In Region 3 the tapered wiggler described above may be used to produce a decelerating bucket that will further decrease the energy of the electrons. This process is depicted in Figs. 5.2(d) and 5.2(e). Regions 4 and 5 are the reverse of Regions 1 and 2 respectively which results in the detrapping of the decelerated electrons at an energy substantially below the original injected energy with only a small increase in the energy spread.

In order that a large fraction of the electrons be decelerated and hence that they transfer energy into the optical field for the operational modes of the FEL described above, the energy spread of the incoming electron beam must be less than the maximum bucket height. This often places a severe restriction on the quality of the electron beam or requires a large laser intensity. To solve this problem we will discuss another technique used in accelerators called phase area displacement.[11]

The method of phase area displacement can cause all of the electrons to be decelerated even when the initial energy spread (or effective energy spread when transverse emittance and magnetic field variation with beam size are included) is considerably larger than the bucket height. Phase area displacement refers to an operational mode in which an empty bucket is <u>accelerated</u> through the phase area of the beam with the result that the phase area occupied by the electrons is displaced <u>downward</u> in energy. An accelerating bucket decelerates the particles. Consider the case where the accelerating bucket starts with a resonant energy far below the energy of the electrons in the beam and is adiabatically moved through the beam until the final resonant energy is far above the electron's energy, as illustrated in Fig. 5.3. Note that for an accelerating bucket $\psi_r < 0$. The final mean energy of the electrons is lowered by the phase area of the empty accelerating bucket divided by 2π, while the final energy spread of the beam is nearly equal to the initial energy spread, i.e.,

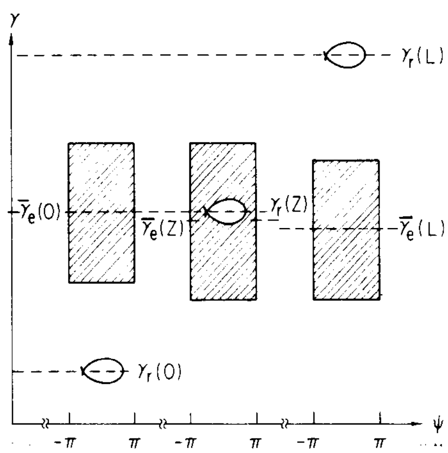

Fig. 5.3. Phase displacement. Position of empty bucket and phase area of electrons at various positions in the FEL.

$$\left[\bar{\gamma}(0) - \bar{\gamma}(L)\right] = \frac{1}{2\pi} J \tag{5.5}$$

and

$$\Delta\gamma_f \sim \Delta\gamma_i \tag{5.6}$$

where J is the area enclosed by the accelerating bucket. From Fig. 5.3, we see that the total change in γ_r must be larger than the sum of the bucket height and the energy spread in the beam, i.e.,

$$|\gamma_r(L) - \gamma_r(0)| \sim |\gamma_r' L| > 2(\delta\gamma)_{max} + \Delta\gamma_{spread} . \tag{5.7}$$

As long as both the adiabatic condition, which is discussed above, and the above condition are met, the energy spread of the beam is not greatly increased and the average energy loss of the electrons is independent of the initial energy spread.[12]

VI. GAIN-EXPANDED WIGGLER

Another scheme[13] designated as a gain-expanded wiggler was proposed by the Stanford Group to reduce the sensitivity of the optical gain to the electron energy. The equations of motion were presented by Madey and Taber at the last conference in Telluride,[14] and a more complete review will be presented by Kroll at this conference. In addition, Madey and Ekstein have obtained new results[15] on the excitation-canceling FEL with a gain-expanded wiggler. In this section we will demonstrate the similarity between the study of synchrobetatron coupling in an accelerator and the study of the gain-expanded FEL. We will see how one can use the results of accelerator orbit theory to derive the equations of motion for the gain-expanded FEL.

The gain-expanded FEL utilizes a transverse gradient in the wiggler magnetic field which has the property that the average value of the dispersion in the wiggler is constant and non-zero. Thus different energy electrons will have different equilibrium trajectories as illustrated in Fig. 6.1. The constant $\bar{\eta}$ is defined by averaging over the oscillatory excursions which have the wavelength of the wiggler.

$$\Delta\bar{x} = \bar{\eta}\,\frac{\delta\gamma}{\gamma}\ . \tag{6.1}$$

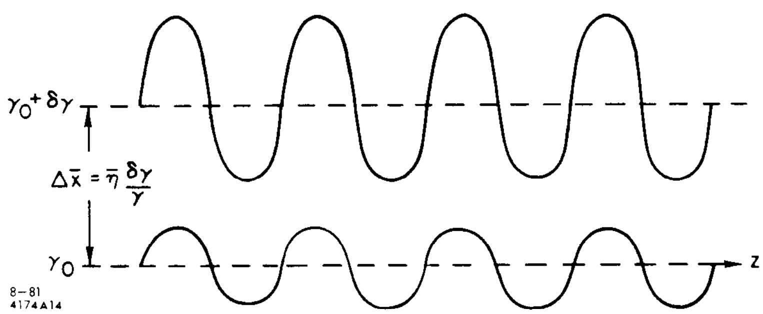

Fig. 6.1. Trajectories for electrons with different energies in gain-expanded wiggler.

For the gain-expanded wiggler the gradient of the wiggler field is chosen so that the increase in the path length, due to the increased magnetic field experienced by the higher energy electrons, just compensates for the increase in the electron speed, i.e.,

$$\frac{\Delta L}{L} = \frac{\Delta v}{v}\ . \tag{6.2}$$

This is to be contrasted with the nongain-expanded wiggler (Fig. 3.3) where the dispersion is zero and the path length decreases with energy. Regardless of their energy, electrons entering on their equilibrium orbits will travel through the gain-expanded wiggler at the same average rate and thus the average rate of change in the relative phase between the transverse electron velocity and the optical wave is independent of energy just as it is for particles at transition energy in an accelerator [Eq. (2.4)].

An electron which enters the wiggler off its equilibrium orbit (in position or angle) will not follow the trajectory described in Fig. 6.1 but will perform a "betatron" oscillation about its equilibrium orbit. This betatron oscillation consists of a rapid oscillation, with a wave number equal to the wiggler wave number k_w, superimposed upon a slow oscillation with a wave number k_β to be deduced later. The transverse motion of both an electron traveling on its equilibrium orbit and an electron executing betatron oscillations about its equilibrium orbit are shown in Fig. 6.2. If we define $\bar{x} = 0$ for the electron with energy γ_o then the averaged equilibrium orbit [in the sense of Eq. (6.1)] of an electron with energy $\gamma = \gamma_o + \delta\gamma$ is given by $\bar{x}_e = \bar{\eta}(\delta\gamma/\gamma)$. The averaged transverse displacement, i.e., ignoring the rapid oscillations at the wiggler frequency, is the sum of the averaged betatron displacement and the averaged equilibrium orbit displacement, i.e.,

$$\bar{x}(z) = \bar{x}_\beta(z) + \bar{\eta}(\delta\gamma/\gamma_o) . \tag{6.3}$$

Now because of the gradient present in the wiggler magnet the particle following such a trajectory experiences an averaged transverse focusing force proportional to the averaged betatron displacement, i.e.,

$$\bar{x}'' = - k_\beta^2 \bar{x}_\beta . \tag{6.4}$$

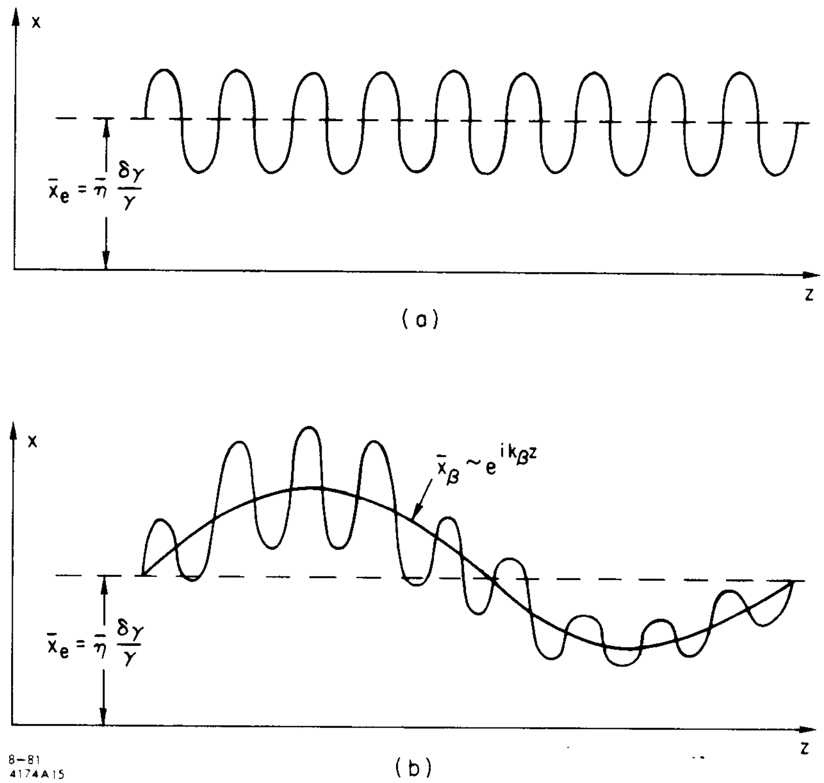

Fig. 6.2. Trajectories for electrons with as a function of betatron oscillation amplitude: (a) $\bar{x}_\beta = 0$; and (b) $\bar{x}_\beta \neq 0$.

This equation actually defines k_β and will be connected with the wiggler field below.

If we substitute from Eq. (6.3) for $\bar{x}$ and allow γ to be a function of z we obtain

$$\bar{x}''_\beta + k_\beta^2\,\bar{x}_\beta = \bar{\eta}(\delta\gamma/\gamma_o)'' \,. \qquad (6.5)$$

The path length traveled by the particle depends upon the averaged betatron displacement as may be seen by careful scrutiny of Fig. 6.2(b). In the positive part of the averaged betatron displacement the electron experiences a higher wiggler magnetic field so that the amplitude of its rapid oscillation and hence the average path length it travels is larger than in the negative part where the amplitude of its rapid oscillation is smaller. Since the speed of the particle is independent of the betatron displacement the average rate of change in the phase variable ψ will then be proportional to the averaged betatron displacement. We will derive the equation for $d\psi/dz$ below, and this equation will be discussed by Kroll later in the conference in more detail.

Equation (6.5) is that of a driven oscillator and if the frequency of the change in the energy variable is near the betatron wave number, then it is possible for the energy oscillations to excite the transverse betatron oscillations. The same kind of equation appears in circular accelerators when the longitudinal or synchrotron motion of the particles is somehow coupled to the transverse betatron motion.[16] The coupling is strongest at a synchrobetatron resonance where there is a correlation between the betatron oscillation frequency, the synchrotron oscillation frequency and the revolution frequency.

An example is illustrated in Fig. 6.3 where a particle enters an accelerating cavity on its equilibrium orbit with energy γ_1 and gains energy from the cavity field so that the particle exits with energy γ_2. After the particle exits the cavity, it discovers that it is not on the proper equilibrium orbit for its new energy, and it will start to execute betatron motion about its new equilibrium orbit. If the betatron frequency is synchronized with the oscillation frequency of the energy then on successive passages this process can build up and a resonance occurs where the transverse betatron motion is driven by the longitudinal energy oscillations.

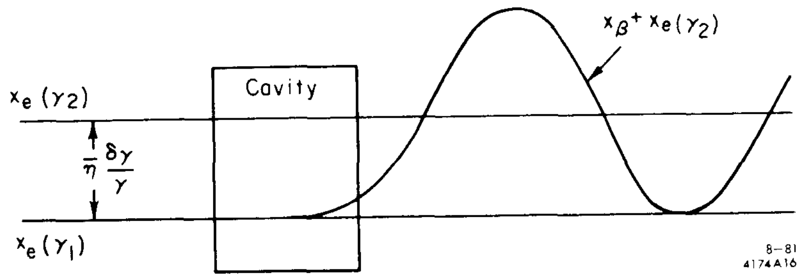

Fig. 6.3. Excitation of transverse betatron motion due to change in particle energy passing through an rf cavity.

As an illustration of how accelerator orbit theory may be used to study the gain-expanded FEL we consider the original magnetic field used by Madey and Taber[14] which has only a $\hat{y}$ component.

$$B_y = \sqrt{2}\, B_w(1 + kx) \sin k_w z + B_c(1 + sx) \; . \qquad (6.6)$$

We use the Lorentz force $F_x = (e/c)v_z B_y$ along with definitions $b_c \equiv \left(eB_c/mc^2\right)$ and $a_w \equiv \left(eB_w/k_w mc^2\right)$ to obtain the following equation of motion for the transverse displacement.

$$x'' + \left[C_0 + C_1 \sin k_w z\right]x = \left[D_0 + D_1 \sin k_w z\right] , \qquad (6.7)$$

where

$$C_0 = -\frac{sb_c}{\gamma} , \qquad (6.8)$$

$$C_1 = -\frac{\sqrt{2}\, k\, k_w\, a_w}{\gamma} , \qquad (6.9)$$

$$D_0 = \frac{b_c}{\gamma} , \qquad (6.10)$$

and

$$D_1 = \frac{\sqrt{2}\, k_w a_w}{\gamma} . \qquad (6.11)$$

Equation (6.7) is a common equation used by accelerator orbit theorists on a daily basis. For example, the terms C_0 and C_1 would represent the quadrupole focusing magnets in a circular accelerator while the terms D_0 and D_1 would represent the dipole steering magnets. The standard method to solve Eq. (6.7) for x(z) is to represent x as the sum of two functions,

$$x(z) = x_\beta(z) + x_e(z) \qquad (6.12)$$

where x_β is the solution to the homogenous part of Eq. (6.7) while x_e is the solution to the general equation with the constraint $x_e(z + \lambda_w) = x_e(z)$. We see that x_β represents the betatron motion while x_e represents the equilibrium orbit discussed above.

For the case where the wiggler wave number is large compared to the betatron wave number, i.e., $k_w >> k_\beta$, the approximate solution to Eq. (6.7) may be derived by a "smooth approximation technique".[17] This technique gives

$$x_e = \frac{1}{k_\beta^2 k_w^2} \left\{ \left[k_w^2 D_0 + \frac{1}{2} C_1 D_1 \right] + \left[C_1 D_0 - C_0 D_1 \right] \sin k_w z \right\} \qquad (6.13)$$

and

$$x_\beta = x_{\beta o} e^{ik_\beta z}\left[1 + \frac{C_1}{k_w^2} \sin k_w z\right] \tag{6.14}$$

with

$$k_\beta^2 = \left[C_0 + \frac{C_1^2}{2k_w^2}\right] \tag{6.15}$$

where the terms we have neglected are of the order of (k_β^2/k_w^2) times the terms we have retained. To verify the validity of the smooth approximation it must be shown _a posteriori_ that $k_\beta \ll k_w$ of course. We see that solutions x_e and x_β each contain a slow oscillating part and a rapid oscillating part, and since the values of C_0, C_1, D_0, and D_1 are functions of the energy the solutions for x_e and x_β are also functions of the energy. This is illustrated in Figs. 6.1 and 6.2.

We choose the value of $\bar{x}_e$ (x_e with the fast oscillations averaged out) to be zero when the energy equals γ_o, by requiring for $\gamma = \gamma_o$.

$$C_1 D_1 = - 2k_w^2 D_0 \tag{6.16}$$

which yields

$$b_c = \frac{k a_w^2}{\gamma_o} . \tag{6.17}$$

With this constraint on the value of B_c we can rewrite Eq. (6.13) through first order in $\delta\gamma/\gamma_o$ as

$$x_e = \frac{1}{k-s}\frac{\delta\gamma}{\gamma_o} - \frac{\sqrt{2}\, a_w}{k_w \gamma_o}\left[1 + \frac{s}{k-s}\frac{\delta\gamma}{\gamma_o}\right] \sin k_w z \tag{6.18}$$

and

$$x_e' = -\frac{\sqrt{2}\, a_w}{\gamma_o}\left[1 + \frac{s}{k-s}\frac{\delta\gamma}{\gamma_o}\right]\cos k_w z \;. \tag{6.19}$$

The average dispersion, defined by $\bar{\eta} = \bar{x}_e/(\delta\gamma/\gamma_o)$ is given by

$$\bar{\eta} = \frac{1}{k-s} \tag{6.20}$$

while the betatron wave number is given by

$$k_\beta^2 \approx \frac{k(k-s)a_w^2}{\gamma_o}\left[1 + (2k-s)\bar{\eta}\,\frac{\delta\gamma}{\gamma_o}\right] . \tag{6.21}$$

In one wiggler period, the path length traveled by an electron on its equilibrium orbit is greater than the distance traveled by the optical wave and depends upon the amplitude of the rapid oscillation of the equilibrium orbit, see Eq. (3.5), through the equation

$$\frac{L - \lambda_w}{\lambda_w} = \frac{1}{2}\,\overline{(x_e')^2} \tag{6.22}$$

where the average is over one wiggler period. By combining Eqs. (3.4), (6.19) and (6.22) we obtain for the average rate of change in the phase ψ of an electron traveling on its equilibrium orbit through first order in $\delta\gamma/\gamma_o$.

$$\frac{d\psi}{dz} = \left[k_w - \frac{k_s}{2\gamma_o^2}\left(1 + a_w^2\right)\right] + \frac{k_s}{\gamma_o^2}\left[1 - \frac{s}{k-s}\, a_w^2\right]\frac{\delta\gamma}{\gamma_o} \;. \tag{6.23}$$

For the gain-expanded wiggler we demand that the value of $d\psi/dz$ be independent of energy which requires that

$$\frac{k-s}{s} = a_w^2 \, . \tag{6.24}$$

By expanding Eq. (6.14) to first order in $\delta\gamma/\gamma_o$ we obtain

$$x_\beta = \bar{x}_\beta \left\{1 - \frac{\sqrt{2}\, ka_w}{k_w\gamma_o}\left[1 - \frac{\delta\gamma}{\gamma_o}\right] \sin k_w z\right\} \tag{6.25}$$

and

$$x'_\beta \approx \bar{x}'_\beta - \frac{\sqrt{2}\, ka_w}{\gamma_o}\, \bar{x}_\beta \left(1 - \frac{\delta\gamma}{\gamma_o}\right) \cos k_w z \tag{6.26}$$

where again we have neglected terms in Eq. (6.26) of order k_β/k_w compared to unity. For the case where the electron is not on its equilibrium orbit but is performing betatron oscillations about its equilibrium orbit the extra distance traveled by the electron is given by

$$\frac{L - \lambda_w}{\lambda_w} = \frac{1}{2}\, \overline{\left(x'_e + x'_\beta\right)^2} \, . \tag{6.27}$$

We combine Eqs. (3.4), (6.19), (6.26) and (6.27) along with the constraint Eq. (6.24) to obtain the average rate of phase change for an electron performing betatron oscillations

$$\frac{d\psi}{dz} = q - \frac{k_s\, k\, a_w^2}{\gamma_o^2}\, \bar{x}_\beta \tag{6.28}$$

$$+ \text{ higher order terms in } \left(\bar{x}_\beta,\ \bar{x}'_\beta \text{ and } \delta\gamma/\gamma_o\right)$$

where

$$q = \left[k_w - \frac{k_w}{2\gamma_o^2}\left(1 + a_w^2\right)\right] = k_w\left[1 - \frac{\gamma_r^2}{\gamma_o^2}\right] . \tag{6.29}$$

The equation of motion for $\bar{x}$ may be obtained from Eq. (6.7) by the smooth approximation which yields

$$\bar{x}'' + k_\beta^2 \, \bar{x} = \left[D_0 + \frac{C_1 \, D_1}{2k_w^2}\right] \tag{6.30}$$

where k_β is given by Eq. (6.15).

If we use the definitions for the C's and D's from Eq. (6.8) to Eq. (6.11) and the constraint from Eq. (6.17) we obtain for the driving term in Eq. (6.30)

$$\left[D_0 + \frac{C_1 \, D_1}{2k_w^2}\right] = \frac{k \; a_w^2}{\gamma} \left[\frac{1}{\gamma_o} - \frac{1}{\gamma}\right] \tag{6.31}$$

and for the focusing term in Eq. (6.30)

$$k_\beta^2 = \frac{k \; a_w^2}{\gamma} \left[\frac{k}{\gamma} - \frac{s}{\gamma_o} \right] . \tag{6.32}$$

To first order in $\delta\gamma/\gamma_o$ we have for the driving term

$$\left[D_0 + \frac{C_1 \, D_1}{2k_w^2}\right] = k_\beta^2 \, \bar{\eta} \, \frac{\delta\gamma}{\gamma_o} \tag{6.33}$$

where we have used the definition of $\bar{\eta}$ given by Eq. (6.20). Thus to first order in $(\delta\gamma/\gamma_o)$ the equation of motion for the average value of the transverse displacement may be written as

$$\bar{x}'' + k_\beta^2[\bar{x} - \bar{\eta}(\delta\gamma/\gamma_o)] = 0 . \tag{6.34}$$

From the definition of $\bar{x}_\beta$ [Eq. (6.3)] we see that this agrees with the desired equation of motion [Eq. (6.5)] for the gain-expanded FEL, namely

$$\bar{x}_\beta'' + k_w^2 \, \bar{x}_\beta = - \eta(\delta\gamma/\gamma_o)'' . \tag{6.35}$$

The remaining equation of motion for the rate of change for the energy variable does not explicitly depend upon the transverse betatron motion (except for a rapid flutter term in the phase which we have ignored) and is given by Eq. (3.14), namely

$$\gamma' = -\frac{k_s a_s a_w}{\gamma} \sin \psi \, . \tag{6.36}$$

The complete set of the equations of motion that describe the motion of electrons traveling through the gain-expanded FEL consists of Eqs. (6.28), (6.35) and (6.36). These equations are essentially the same as those derived by Madey and Taber[14] and may be compared directly with Eqs. (64) of their paper by replacing their expressions by the following equivalent expressions used in this paper.

$$\left[\frac{\gamma_o \lambda_q}{\sqrt{2}\, 2\pi\, \rho_o} \right] \rightarrow a_w \, , \tag{6.37}$$

$$\frac{e|\mathcal{E}|}{mc^2} \rightarrow \sqrt{2}\, k_s\, a_s \, , \tag{6.38}$$

$$(k-s) \rightarrow \frac{1}{\bar{\eta}} \, , \tag{6.39}$$

and

$$k(k-s)\left(\frac{\lambda_q}{\sqrt{2}\, 2\pi\, \rho_o}\right)^2 \rightarrow k_\beta^2 \, . \tag{6.40}$$

For the case of the gain-expanded wiggler where the magnetic field and wave number are independent of the longitudinal coordinate z the reference energy γ_o is independent of z and we can rewrite Eq. (6.36) to first order in $\delta\gamma/\gamma_o$ as

$$\left(\frac{\delta\gamma}{\gamma_o}\right)' = -\frac{k_s a_s a_w}{\gamma_o^2} \sin \psi . \qquad (6.41)$$

We also can use the constraint Eq. (6.24) to rewrite Eq. (6.28) to lowest order in $\bar{x}_\beta$ and $\delta\gamma/\gamma_o$ as

$$\psi' = q - \frac{k_s(1 + a_w^2)}{\bar{\eta}\, \gamma_o^2} \bar{x}_\beta . \qquad (6.42)$$

If we take the derivative of Eq. (6.41) and substitute it into Eq. (6.35) we obtain the following equation for $\bar{x}_\beta$

$$\ddot{\bar{x}}_\beta + (k_\beta^2 - \Omega_L^2 \cos \psi)\bar{x}_\beta = -\frac{q k_s \bar{\eta}\, a_s a_w}{\gamma_o^2} \cos \psi$$

(6.43)

where we have used the fact that $\gamma_o \approx \gamma_r$ to write

$$\frac{k_s^2(1 + a_w^2)a_s a_w}{\gamma_o^4} \approx \frac{4k_w^2 a_s a_w}{(1 + a_w^2)} = \Omega_L^2 . \qquad (6.44)$$

There are two regimes where self consistent solutions to Eqs. (6.42) and (6.43) may be obtained analytically. One is where $\Omega_L^2 \ll k_\beta^2$ and the other where $\Omega_L^2 \gg k_\beta^2$. The character of these solutions is very different in the two regimes as will be discussed by Kroll later in the conference.

Note for a small initial value of $\bar{x}_\beta$ that when $\cos \psi$ is less than zero (i.e., $|\psi| > \pi/2$) $\bar{x}_\beta$ increases and becomes positive. As we see from Fig. 6.2 or Eq. (6.42) for positive value of $\bar{x}_\beta$ the path length traveled by the electron increases and the relative phase ψ decreases. On the other hand, when $\cos \psi$ is greater than zero (i.e.,

$|\psi| < \pi/2$) then $\bar{x}_\beta$ decreases and becomes negative so that the path length traveled by the electron decreases and ψ increases. The excitation of betatron oscillations occurs for values of $|\psi| \neq \pi/2$ and produces a migration of the electron towards a value of $\psi = \pi/2$. From Eq. (6.41) we conclude that this tendency for the electrons to bunch at a phase near $\psi = \pi/2$ will also produce a net deceleration of the electrons. The strong bunching of the electrons occurs whenever the oscillation frequency of the driving term [cos ψ in Eq. (6.43)] is near the betatron frequency, i.e., when $q \approx k_\beta$. Thus a gain-expanded wiggler uses the transverse betatron motion, instead of the energy motion (as in the nongain-expanded FEL) to provide the necessary bunching of the electrons to transfer energy to the optical wave.

Further treatment of the gain-expanded FEL may be found elsewhere[18] and in the presentation by N. M. Kroll later in this conference.

ACKNOWLEDGMENTS

It is a pleasure to acknowledge the work of my colleagues Drs. N. M. Kroll and M. N. Rosenbluth with whom I had the pleasure to share several summer workshops on free-electron-lasers in La Jolla. I would like to thank Drs. A. W. Chao, R. K. Cooper and J. R. Rees for reading the paper and suggesting many improvements. Marge Barnes and the SLAC Publications Department were both very helpful in preparing this manuscript. Also, I would like to thank Drs. G. T. Moore, H. S. Pilloff and M. O. Scully for the chance to attend the last two FEL Conferences and for the opportunity to present this paper.

REFERENCES

1. L. R. Elias, W. M. Fairbank, J. M. J. Madey, H. A. Schwettman, and T. I. Smith, Phys. Rev. Lett. 35, 717-720 (1976).
2. Proceeding of the Telluride Conference, Physics Quantum Electronics, Vol. 5, August 1977.
3. See for example, F. A. Hopf, P. Meystre, G. T. Moore, and M. O. Scully, ibid, pp. 41-113; and N. M. Kroll, ibid, pp. 115-156.
4. W. B. Colson, ibid, pp. 157-196.
5. Much of the material for this review paper has been taken from the results of the work: N. M. Kroll, P. L. Morton, and M. N. Rosenbluth, IEEE J. Quantum Electronics, QE-17, No. 8, 1436-1468 (1981).
6. Proceeding of the Telluride Conference, Physics Quantum Electronics, Vol. 7, August 1979.
7. See for example, K. R. Symon, and A. M. Sessler, CERN Symposium, Vol. 1, June 1956, pp. 44-58.
8. J. M. J. Madey, Nuovo Cimento 50B, 64-88 (1976).
9. A. Renieri, Nuovo Cimento 53B, 160-178 (1979).
10. D. A. G. Deacon, Ph.D. Thesis, Stanford University (1976).
11. D. A. Swenson, Proceeding of the International Conference on High Energy Acceleration, BNL, September 1979, pp. 160-178.
12. For a more detailed treatment of this technique, see N. M. Kroll, P. L. Morton, and M. N. Rosenbluth, Proceeding of the Telluride Conference, Physics Quantum Electronics, Vol. 7, August 1979, pp. 104-109.
13. T. I. Smith, J. M. J. Madey, L. R. Elias and P. A. G. Deacon, J. Appl. Phys. 50, 4580 (1979).

14. J. M. J. Madey and R. C. Taber, Proceeding of Telluride Conference, Physics Quantum Electronics, Vol. 7, August 1979, pp. 741-777.

15. J. M. J. Madey and J. N. Eckstein, Internal HEPL Report, Stanford, California (1981).

16. SPEAR Group, IEEE Trans. Nucl. Sci. NS-22, No. 3, 1863-1865 (1977).

17. K. R. Symon, D. W. Kerst, L. W. Jones, L. J. Laslett, and K. M. Terwilliger, Phys. Rev. 103, 1837-1859 (1956).

18. N. M. Kroll, P. L. Morton, M. N. Rosenbluth, J. N. Eckstein, and J. M. J. Madey, IEEE J. Quantum Electronics QE-17, No. 8, 1496-1507 (1981).